CCGP Coal Combustion and Gasification Products

ISSN 1946-0198

journal homepage: www.coalcgp-journal.org

Separation of Unburned Carbon from Coal Conversion Ash: Development and Assessment of a Dry Method

Charlotte J. Badenhorst[1,*], Nicola J. Wagner[1], Bruno R.V. Valentim[2], Karel S. Viljoen[1], Ana C. Santos[2], Alexandra Guedes[2]

[1] CIMERA Department of Geology, University of Johannesburg, PO Box 524, Auckland Park, Johannesburg, 2006, South Africa
[2] Instituto de Ciências da Terra (ICT), Pólo da Faculdade de Ciências da Universidade do Porto, e Departamento de Geociências, Ambiente e Ordenamento do Território, Faculdade de Ciências, Universidade do Porto, Rua do Campo Alegre, S/N, 4169-007 Porto, Portugal

A B S T R A C T

Unburned carbon found in coal conversion ash has the potential to be used in a variety of value-added applications. However, it is first necessary to separate the unburned carbon from the rest of the ash phases. This poses challenges due to the relatively low starting carbon-in-ash values (0.4 to 7.8 wt% reported for South African sources), and the high carbon grades (ideally ~90 wt% carbon) and recoveries that need to be achieved.

In this study a dry method for the separation of unburned carbon from coal ash was developed and assessed using fly, bottom, and gasification ash samples obtained from various South African coal conversion utilities. The idea is to subsequently use the unburned carbon product as a precursor for synthetic graphite manufacturing. The separation consisted of a combination of size, electrostatic (CoronaStat), and magnetic separation steps, and the carbon grades (as loss on ignition [LOI]) and recoveries were assessed for each step. Precharacterization included X-ray diffraction, LOI, and petrography (carbon-mineral associations) analyses.

The carbon grades increased from 4.01 and 7.04 wt% to 56.55 and 65.74 wt%, respectively, for two fly ash samples. The process was less efficient for the bottom and gasification ash samples, where final carbon grades of 53.21 and 45.10 wt% were achieved from a starting base of 5.47 and 6.90 wt%, respectively. The carbon recoveries for all samples were low (<35%), possibly due to the mineral inclusions that form part of the carbon matrix.

The suggested separation method is promising but still requires further modification.

A R T I C L E I N F O

Article history: Received 4 February 2019; Received in revised form 15 April 2019; Accepted 7 May 2019

Keywords: South Africa; coal; petrography; XRD; Corona electrostatic separation

1. Introduction

Carbon-based products are at the forefront of technological development. Examples include activated carbon for water and gas purification, carbon and lamp black found in the printing industry, synthetic graphite for electrodes and lubricants, and carbon-carbon composites in the aviation and space sciences (Pierson, 1993). Unburned carbon found in coal conversion ash may be a suitable source of carbon for some of these applications. In particular, the production of synthetic graphite requires attention, because natural graphite is considered to be a scarce commodity, and therefore any synthetic alternative is desirable (European Commission, 2017).

More than 780 million metric tons of coal conversion ash are produced annually worldwide, with more than 34 million metric tons produced in South African alone (Heidrich et al., 2013; Reynolds-Clausen and Singh, 2017). A large proportion of the ash finds application in the cement and concrete industries, where ASTM regulation restricts the unburned carbon percentage to a maximum of 6 wt% loss on ignition (LOI) to prevent adsorption of air-entraining agents (ASTM C618-17a [ASTM International, 2017]). Industrial

* Corresponding author. *E-mail:* charlotte.cb82@gmail.com

doi: 10.4177/CCGP-D-19-00002.1

Table 1
Sample identification, type, origin, and mass

	Sample type	Sample origin	Mass obtained (kg)
Power station 1			
FA PS1	Fly ash	Eskom power utility	13
BA PS1	Bottom ash	Eskom power utility	10
Power station 2			
FA PS2	Fly ash	Eskom power utility	7
Gasification utility			
GA East	Gasification ash	Sasol Synfuels	23

separation processes exist for the lowering of the LOI levels in ash, such as dry electrostatic separation (Bittner et al., 2014). However, to extract the unburned carbon for use in synthetic graphite production, the process is far more complicated due to the typical low carbon-in-ash percentages and the high grades and recoveries needed for usage. LOI percentages for South African power utility ash range between 0.4 and 7.8 wt%, and Matjie et al. (2005, 2008) reported LOIs of 5, 5.8, and 8.2 wt% for South African gasification ash.

This article focuses on the extraction of unburned carbon from fly ash, bottom ash, and gasification ash from select South African utilities, using a combination of techniques to increase the efficiency and effective separation of the unburned carbon from the mineral component. The aim was to produce a carbon-rich fraction that could be used as a precursor for synthetic graphite and subsequently immobilized on electrode surfaces and tested in energy-related reactions such as the hydrogen evolution reaction (HER), oxygen evolution reaction (OER), oxygen reduction reaction (ORR), and water splitting (simultaneous H_2 and O_2) reactions. For this reason, a dry method was needed where the unburned carbon pores cannot be occluded. Therefore, separation techniques such as froth flotation, oil agglomeration, and sink-float using other liquids than water were not suitable. A dry scheme consisting of size, electrostatic, and magnetic separation was thus used. It is noted that the methods used were not novel. However, the design and assessment of the separation process for this specific batch of samples and for this specific end use are novel. Ideally, 90 wt% LOI was sought with a high carbon recovery.

2. Methods

2.1. Samples and preparation procedures

Fly ash (FA), bottom ash (BA), and gasification ash (GA) were supplied in 2016 by two South African combustion utilities and one gasification utility (Table 1), following in-house sampling procedures based on ISO 13909-2 (International Organization for Standardization [ISO], 2016). The samples provide a snapshot in time of the ash produced by the utility. The feed coal to the combustion and gasification processes is medium rank C bituminous, typically poor in vitrinite (below 30%) and high in mineral matter (ash contents above 20%), originating from the Witbank and Highveld Coalfields.

The bulk ash samples were air dried and divided into smaller, representative fractions. A representative sample from each parent ash was characterized in detail, and the remainder of the sample was utilized in the separation trials. Owing to the coarser sizes of the bottom and gasification ash samples, these samples were pulverized before characterization commenced.

2.2. Sample characterization

The mineralogical compositions of the ash samples were determined by X-ray diffraction (XRD). A PANalytical Empyrean diffractometer with PIXcel detector and fixed slits with Fe filtered Co-K$^{\infty}$ radiation was used for detection, and the X'Pert Highscore plus software was used for phase identification. The Rietveld method was used to semiquantify the data, and the amorphous percentages were determined by adding a 20% Si standard to the samples.

The LOI analysis was conducted by MAK Analytical (South Africa). The samples were heated in an oxidized atmosphere to 500°C, maintaining this temperature for 30 minutes before being heated to 815°C. The samples were kept at 815°C for 60 minutes before the mass loss was determined. Conversion of the mass loss to a percentage provides the LOI value.

Petrography enabled the visible assessment of the mineral-carbon associations in the carbon-ash particles. The samples were crushed to <1 mm (where necessary), mounted in epoxy resin, and polished according to ISO 7404 part 2 (ISO, 2009). A Zeiss Imager M2M reflected light microscope with an oil immersion objective and a combined magnification of $\times 500$ was used.

2.3. Separation trials

A schematic of the separation stages followed is provided in Figure 1. A dry sieving technique was used to separate the ash samples into different size fractions using three different sieve columns: fly ash: 38, 53, 75, 106, 150, 212 µm bottom ash: 75, 150, 300, 600, 1000, 2000 µm and gasification ash: 150, 300, 600, 1000, 2000, 5000 µm. The sieve stack was loaded with 150 g of sample, and mechanically sieved for 20 minutes. The LOI for each size fraction was obtained to determine the inferred carbon purity of the product. Fractions with high LOIs were selected for further separation of the ash and carbon. Particle size separation allows the carbon-richest size fraction to be found, and a large amount of sample with a low carbon content to be discarded.

After the sieving trials, selected size fractions were dried overnight (110°C) in a drying oven before electrostatic separation commenced, to ensure the removal of excess moisture, because this is known to reverse particle charge and cause inefficient separation (Baltrus et al., 2002). A CoronaStat, situated at the University of Pretoria, was used for electrostatic separation. The rotor speed was kept constant at 40 revolutions per minute (rpm). The voltage control was tested at 10, 15, and 20 kV, respectively. The CoronaStat had five collection bins to collect the conductive (C), middlings 1 (M1), middlings 2 (M2), middlings 3 (M3), and nonconductive (NC) particles. The bins with the highest LOIs were selected and passed through the electrostatic separator a second time, under the same conditions, to improve the carbon grades. Triboelectrostatic separation is more sensitive than a CoronaStat electrostatic separator in the separation of minerals with small differences in their electron voltages (Bada et al., 2010). This technology might thus be more efficient at separating unburned carbon from ash (Ban et al., 1997; Maroto-Valer et al., 1999; Gray et al., 2002; Soong et al., 2002). However, a triboelectrostatic separator was unavailable during the

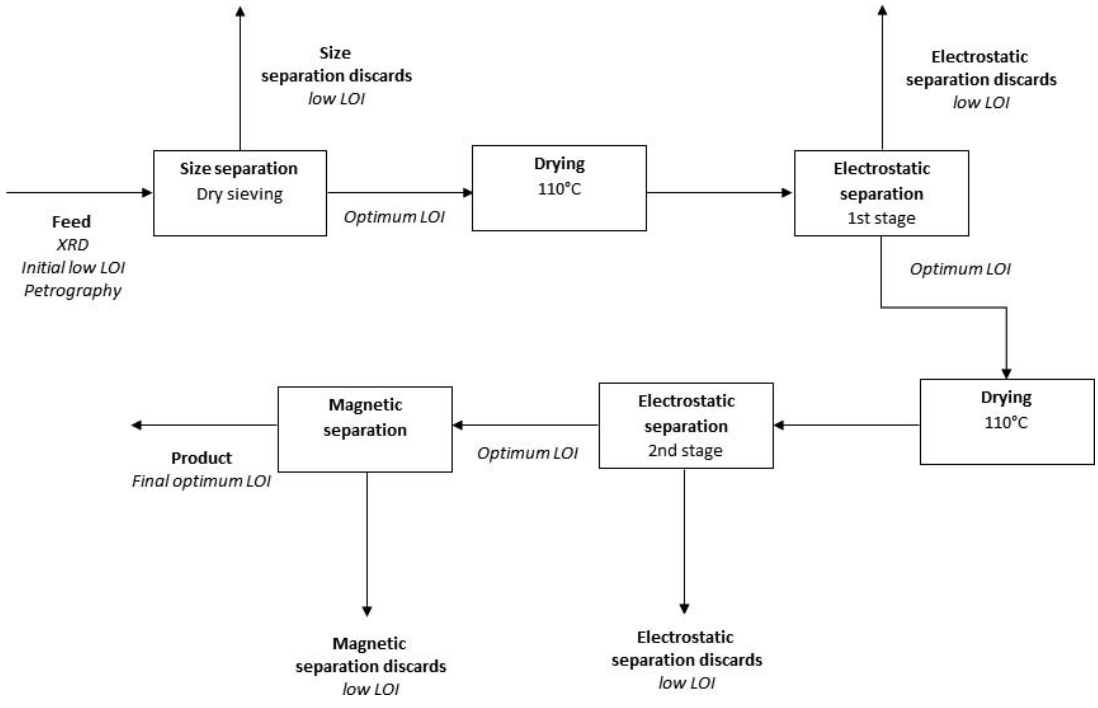

Fig. 1. Schematic of the separation stages followed.

experimental phase of this study, and therefore a CoronaStat was used.

The bins with the highest LOIs were then selected for magnetic separation. A Frantz dry magnetic separator was used, and the magnetic intensity was varied at 0.5, 1.0, and 1.5 A. Although not a commonly used technique, it was found that magnetic separation can remove large amounts of magnetic material from the unburned carbon product. The magnetic fraction can also subsequently be used in value-added applications, e.g., as a catalyst.

2.4. Assessment of separation efficiency

Carbon grade, carbon recovery, and sample yield were used (cumulative basis) (Eq. 1–3) to assess the separation efficiency. Carbon grade indicates the purity of the product stream. LOI was used to determine the carbon grade. Although LOI is a rough estimate of unburned carbon, it is a fast and simple process compared with other carbon determination techniques such as total carbon, carbon speciation, and a microscopic count (Brown and Dykstra, 1995; Fan and Brown, 2001; Mohebbi et al., 2015). Carbon recovery is an indication of how much of the initial carbon mass ends up in the carbon product. Sample yield is an indication of how much of the initial sample mass ends up in the carbon-rich product.

$$\text{Carbon grade (wt\%)} = (\text{Mass of carbon in product stream} \div \text{Mass of total product stream}) \times 100 \quad (1)$$

$$\text{Carbon recovery (\%)} = (\text{Mass of carbon in product stream} \div \text{Mass of carbon in feed stream}) \times 100 \quad (2)$$

$$\text{Sample yield (\%)} = (\text{Mass of product stream} \div \text{Mass of feed stream}) \times 100 \quad (3)$$

3. Results and Discussion

3.1. Parent sample characterization

The mineralogical and LOI results are presented in Table 2. The ash is dominated by quartz and glassy amorphous phases, with relatively high mullite contents. The low LOI values pose possible challenges to obtaining a high-grade carbon product with a suitable recovery.

A microscopic image of a typical carbon particle found in the ash is provided in Figure 2. Minerals (mainly amorphous glass, quartz, and clays) are finely disseminated and appear

Table 2
Mineral composition (XRD) and loss on ignition (LOI) of the samples (wt%)

Phase (wt%)	Formula	FA PS1	FA PS2	BA PS1	GA East
Mullite	$3Al_2O_3 2SiO_2$ or $2Al_2O_3 SiO_2$	15.30	29.70	15.30	14.70
Quartz	SiO_2	52.70	18.66	29.60	12.51
Hematite	Fe_2O_3	0.68	0.95	0.63	0.37
Lime	CaO	0.11	0.30	ND	ND
Cristoballite	SiO_2	0.03	0.10	0.29	0.43
Sillimanite	Al_2SiO_5	0.21	0.67	0.05	0.16
Calcite	$CaCO_3$	0.36	0.05	0.77	0.97
Magnetite	Fe_3O_4	0.43	0.68	0.40	0.41
Plagioclase	$NaAlSi_3O_8$	ND	ND	8.21	12.39
Periclase	MgO	ND	1.41	ND	ND
Amorphous		30.16	47.49	44.74	58.07
Loss on ignition		7.04	4.01	5.47	6.90

Note: ND = not detected.

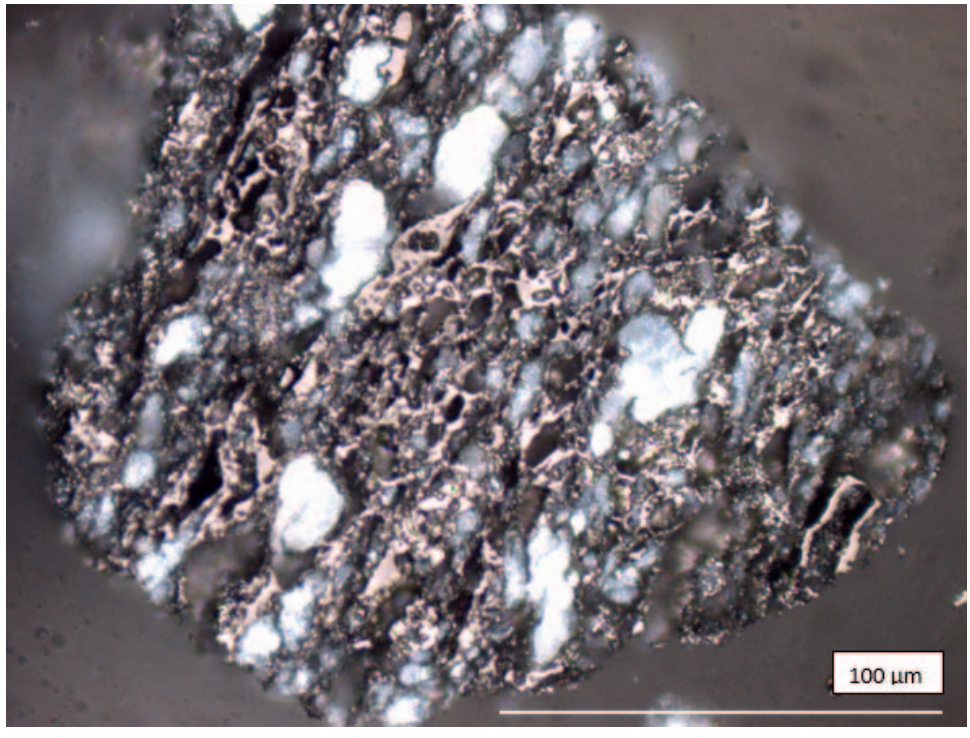

Fig. 2. Typical mineral-carbon associations in fly ash particles (reflected light, ×500 oil objective).

interwoven in the carbon matrix. This intimate association is most likely related to the inertodetrinite-silicate relationship typically found in the Witbank-Highveld feed coals. Inertodetrinite represents small (<10 µm), detrital carbon, and it is usually embedded with finely dispersed quartz and clay minerals (Wagner et al., 2018). To determine whether milling would liberate the carbon, image analysis was applied using a technique proposed by Dorland et al. (2015). It was found that if milling at a size of 20 µm took place, the smaller particles would remain high in mineral matter, essentially a replicate of the original particle. This is referred to as the "mini-me" effect and makes milling in this case impractical (McMillan et al., 2015).

3.2. Particle size separation

During particle size distribution (PSD) determination, it was noted that the coarser fractions of the fly ash samples were darker in color than the finer size fractions (Figure 3). Hence, the coarser fractions are enriched in carbonaceous particles relative to the finer fractions, which is corroborated by the LOI percentages of the fly ash samples that increase with an increase in particle size (Figure 4). Hurt and Gibbins (1995), Külaots et al. (2004), and Lu et al. (2007) found similar results for their separated fly ash samples. As volatile matter evolves, the vitrinite and reactive semifusinite in the coal become plastic, swell, and harden as larger porous char. The macerals in the inertinite-dominant particles devolatilize more selectively with limited pore development, forming large mixed porous chars. Some of these large chars are not completely consumed during the combustion process and therefore end up in the ash as large carbon particles.

No visible trends were apparent with regard to the bottom and gasification ash samples in terms of carbon content and PSD. Thus, size separation was suitable as a preconcentration step for the fly ash samples only. However, in order to use the CoronaStat, particles larger than 600 µm in the bottom ash sample were discarded, losing only 15% of the initial carbon. For the gasification ash sample,

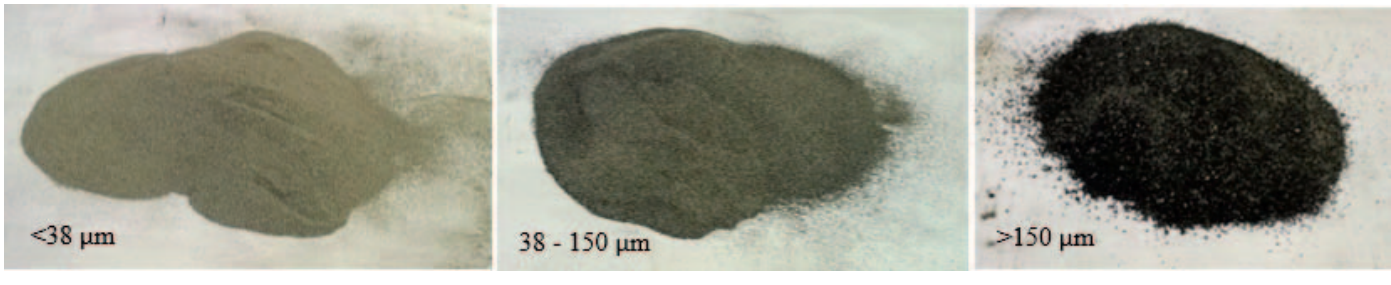

Fig. 3. Visual confirmation of carbon content increase with particle size.

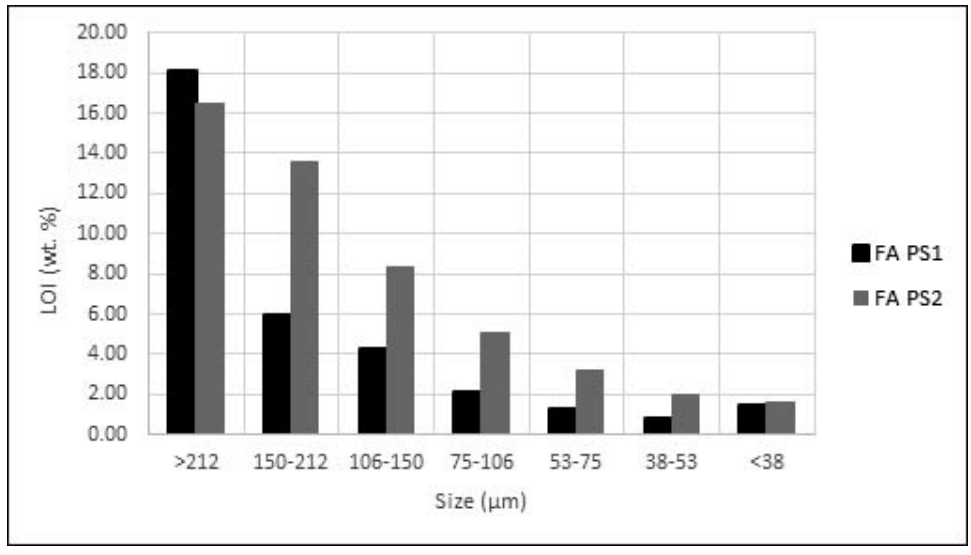

Fig. 4. Loss on ignition (LOI) increase with particle size (fly ash [FA] samples).

the material loss would have been too great if particles larger than 600 µm were discarded; hence, the gasification ash was manually milled to a top size of 600 µm.

The carbon recoveries and sample yields for the fly ash samples were used to determine the size cutoff points (Figure 5). The chosen cutoff point for FA PS1 was 150 µm, and that for FA PS2 was 75 µm. At these cutoff points, the highest grades could be reached without losing too much of the carbon. Hence, all particles larger than 150 and 75 µm, respectively, were used in the subsequent concentration trials. Splitting at the chosen cutoff points resulted in doubling the grades, and removing the bulk of the sample (yield), while at the same time keeping the bulk of the carbon (recovery) (Table 3).

3.3. Electrostatic separation

A voltage setting of 20 kV gave the best results for the fly ash samples. For the bottom and gasification ash samples, a voltage setting of 15 kV was sufficient. In Figure 6, the cumulative grades, recoveries, and yields are given. Bins C and M1 for FA PS1 and FA PS2 provided similar recoveries and yields, and the grades almost tripled their value from the previous size separation stage (Table 3). If only bin C was kept, the grades would have increased substantially, but the recoveries would have been very low.

For the bottom and gasification ash samples, it is very clear that the grades for M1, M2, M3, and NC are more consistent, and only the conductive fraction showed a change in grade. However, the recoveries were very low for this fraction (Table 3).

The selected cutoff point fractions were recycled through the electrostatic system again to give the particles a second chance to separate. For the fly ash samples, the C and M1 fractions were once again separated, while for the bottom and gasification ash samples, only the conductive fraction was used (Table 3). All grades increased when recycled. The most substantial increase was seen for BA PS1. However, the carbon recoveries for the fly ash samples were much higher when compared to the recoveries for the bottom and gasification ash samples.

The electron voltage of carbon is 4 eV, and that of Al-Si minerals (glass) is 4.7–5 eV (Soong et al., 1998). Triboelectrostatic

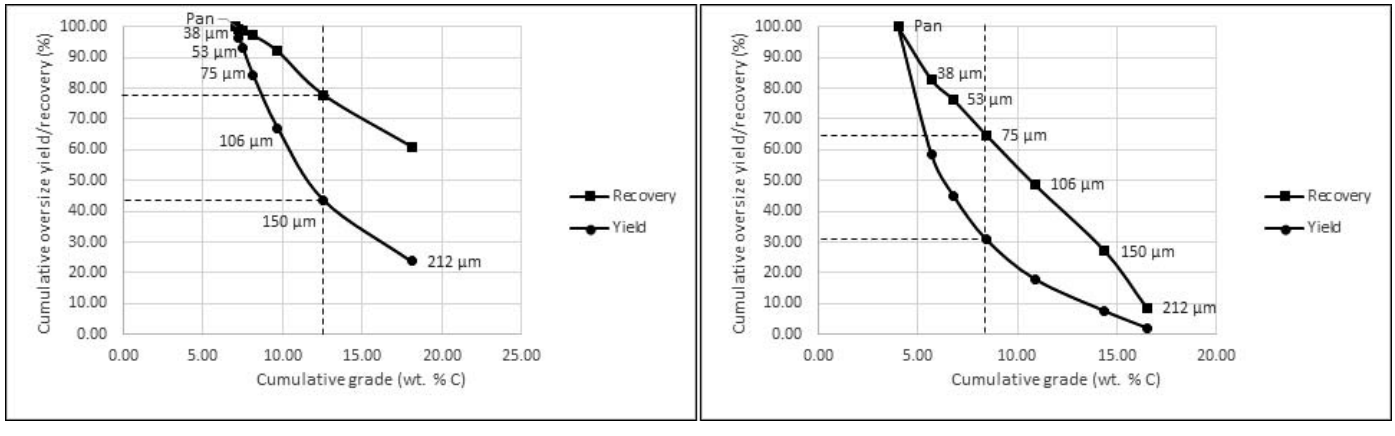

Fig. 5. Cumulative carbon grade, carbon recovery, and sample yield for fly ash (FA) PS1 (left) and FA PS2 (right) at different particle sizes.

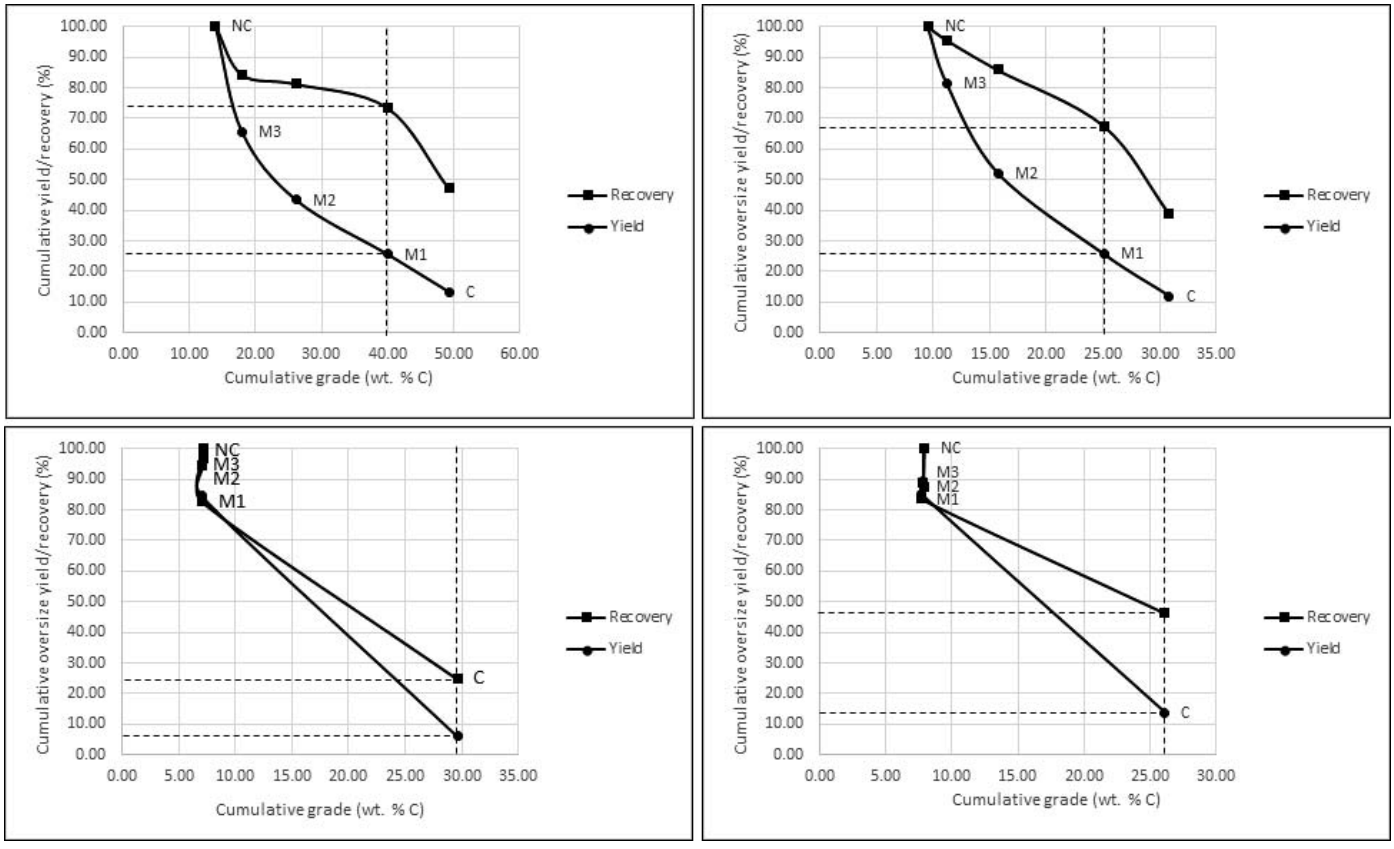

Fig. 6. Cumulative carbon grade, carbon recovery, and sample yield for FA PS1 (top left), FA PS2 (top right), bottom ash (BA) PS1 (bottom left), and gasification ash (GA) East (bottom right) for the different electrostatic bins. FA = fly ash; NC = nonconductive; M1, M2, and M3 = middlings 1, 2, and 3; C = conductive.

Table 3
Carbon grades, carbon recoveries, and samples yields for the separation process flow diagram

	Initial grade (wt% C)	Cutoff point (dependent)	Final grade (wt% C)	Carbon recovery (%)	Sample yield (%)
Size separation					
FA PS1	7.04	+150 μm	12.56	77.86	43.67
FA PS2	4.01	+75 μm	8.44	64.87	30.82
Electrostatic separation first stage[1]					
FA PS1	12.56	M1 and C bins	36.71	72.16	26.10
FA PS2	8.44	M1 and C bins	25.67	68.77	26.96
BA PS1	5.47	C bin	26.88	22.79	6.04
GA East	6.90	C bin	26.80	45.82	13.32
Electrostatic separation second stage[1]					
FA PS1	36.71	M1 and C bins	44.30	73.62	55.86
FA PS2	25.67	M1 and C bins	36.70	78.55	52.43
BA PS1	26.88	C bin	45.17	36.62	24.76
GA East	26.80	C bin	37.12	50.21	31.84
Magnetic separation					
FA PS1	44.30	0.5	65.74	77.36	60.20
FA PS2	36.70	0.5	56.55	50.83	33.65
BA PS1	45.17	0.5	53.21	86.17	76.00
GA East	37.12	1.5	45.10	73.15	62.60
Overall					
FA PS1	7.04	NA	65.74	32.00	3.83
FA PS2	4.01	NA	56.55	17.80	1.47
BA PS1	5.47	NA	53.21	7.19	1.14
GA East	6.90	NA	45.10	16.83	2.65

[1] Five collection bins were used to collect the conductive (C), middlings 1 (M1), middlings 2 (M2), middlings 3 (M3), and nonconductive (NC) particles during electrostatic separation. NA = not applicable.

separation is more sensitive than a CoronaStat electrostatic separator in the separation of minerals with small differences in their electron voltages (Bada et al., 2010). This technology might thus be more efficient at separating unburned carbon from ash. Maroto-Valer et al. (1999) used size separation in combination with triboelectrostatic separation to obtain carbon grades ranging between 88 and 91 vol%, starting from parent fly ash samples with carbon grades ranging between 36 and 39 vol%. Soong et al. (2002) increased their initial fly ash carbon grades (12 and 14 wt%) to a maximum of 60 wt% carbon by using a combination of size and triboelectrostatic separation. Gray et al. (2002) used a double-stage triboelectrostatic separation process to obtain a 35 wt% carbon product from an 18 wt% carbon fly ash sample. Their carbon recovery was below 50%. Ban et al. (1997) used a triboelectrostatic separator to obtain carbon products with grades of up to 50 wt% and recoveries >50% from fly ash samples. Unfortunately, a triboelectrostatic separator was not available during the experimentation phase of this study, and therefore its effect on the samples used in this paper is unknown.

3.4. Magnetic separation

According to Valentim et al. (2016), magnetic material in ash is present as massive or dendritic ferrospheres and as finely dispersed crystals trapped in glassy phases. As a result, a magnetic separation stage was added to the existing separation scheme. Results are included in Table 3. For the fly ash samples, it was found that increasing the magnetic intensity above 0.5 A resulted in a significant drop in recovery without any increase in grade. For the

gasification ash sample, it was found that at 0.5 A, a very low grade but a high recovery were obtained. The magnetic intensity for this sample was therefore increased to 1.5 A. Although the grades increased for the fly ash samples during the magnetic separation step, the carbon recovery for FA PS2 was much lower than for FA PS1. For the bottom and gasification ash samples, the grades did not increase substantially, even after increasing the magnetic intensity. The reason is unclear, considering that the magnetic fractions in the form of hematite and magnetite were similar for the four samples (Table 2).

4. Conclusions

A dry method for the separation of unburned carbon from coal conversion ash was developed and assessed on fly ash, bottom ash, and gasification ash samples obtained from various South African utilities. The aim was to obtain a carbon-rich fraction that could be used in a pregraphitization process as a potential replacement for natural graphite. The formed synthetic graphite could subsequently be used in green energy applications. Ideally, a carbon grade of 90 wt% was sought. The dry separation steps included size, electrostatic (CoronaStat), and magnetic separation. The final (overall) carbon grades, carbon recoveries, and yields are provided in Table 3. The grades increased significantly from the parent samples. Although FA PS1 produced the highest final grade (65.74 wt%), FA PS2 produced the largest increase, with an initial grade of 4.01 wt% and a final grade of 56.55 wt%. The grade for GA East was the lowest at 45.10 wt%.

The overall recoveries were relatively low, possibly related to the unliberated nature of the carbon component. From the microscopic analysis, it was observed that the ash minerals were finely disseminated in the carbon structure and had a "mini-me" arrangement, meaning that even after milling, the smaller particles would remain high in mineral matter, essentially a replicate of the original particle. This excluded milling as an option for mineral liberation. Ultrasonic treatment was applied to see if the inclusions could be "shaken" loose, but this was not successful.

The 90 wt% grade target was not reached, and further experimentation was conducted. This included density separation (sink-float) on FA PS1, after which a final LOI of 82.91 wt% was achieved. It is noted that the quartz content for this sample was exceptionally high (Table 2), and seeing that quartz is very dense (compared with other phases in ash), the density separation was efficient. The recovery, however, was very low. However, because of the expected usage of this carbon product in green energy applications, the carbon pores cannot be occluded, and density separation is thus not feasible.

Acknowledgments

This work forms part of the 3rd ERA-MIN Joint Call (2015) project CHARPHITE, a collaboration among Portugal, Romania, Argentina, Poland, Spain, and South Africa, and the authors would like to acknowledge the different inputs from the different partners.

This work is based on research supported by the National Research Foundation (NRF) of South Africa (grant no. 103466) and the Department of Science and Technology (DST)–NRF ERA-MIN grant for the CHARPHITE project. The authors also acknowledge DST-NRF Centre of Excellence for Integrated Mineral and Energy Resource Analysis (CIMERA) for additional financial assistance; Fundação Ciência e Tecnologia, Portugal (FCT; ERA-MIN/0005/2015); the Institute of Earth Sciences (ICT; FCT UID/GEO/04683/2013); and COMPETE POCI-01-0145-FEDER-007690. K.S. Viljoen acknowledges financial support from the South African DST through their Research Chairs initiative (Geometallurgy), as administered by the NRF. A.C. Santos benefited from a PhD scholarship financed by FCT, Ref. SFRH/BD/131713/2017.

References

ASTM International, 2017. Standard specification for coal fly ash and raw or calcined natural pozzolan for use in concrete. ASTM C618a. In: Annual Book of ASTM Standards, vol. 04.02. ASTM International, West Conshohocken, PA.

Bada, S.O., Falcon, R.M.S., Falcon, L.M., 2010. The potential of electrostatic separation in the upgrading of South African fine coal prior to utilization—a review. The Journal of The Southern African Institute of Mining and Metallurgy 110, 691–702.

Baltrus, J.P., Diehl, J.R., Soong, Y., Sands, W., 2002. Triboelectrostatic separation of fly ash and charge reversal. Fuel 81, 757–762.

Ban, H., Li, T.X., Hower, J.C., Schaefer, J.L., Stencel, J.M., 1997. Dry triboelectrostatic beneficiation of fly ash. Fuel 76(8), 801–805.

Bittner, J.D., Hrach, F.J., Gasiorowski, S.A., Canellopoulus, L.A., Guicherd, H., 2014. Triboelectric belt separator for beneficiation of fine minerals. Procedia Engineering 83, 122–129.

Brown, R.C., Dykstra, J., 1995. Systematic errors in the use of loss-on-ignition to measure unburned carbon in fly ash. Fuel 74(4), 570–574.

Dorland, M.I., Campbell, Q.P., Le Roux, M., Erasmus, P., McMillan, K., Dorland, H.C., 2015. Predicting the washability behaviour of coal by numerical simulation of washabilities and product liberation from photographs. In: Proceedings of the South African Coal Processing Society Conference, Secunda, South Africa, 25–27 August 2015 (De Korte, J., ed.). South African Coal Processing Society, Secunda.

European Commission, 2017. Communication from the Commission to the European Parliament, the Council, the European Economic and Social Committee and the Committee of the Regions on the 2017 List of Critical Raw Materials for the EU. COM (2017) 490 Final. European Commission, Brussels, Belgium.

Fan, M., Brown, R.C., 2001. Comparison of the loss-on-ignition and thermogravimetric analysis techniques in measuring unburned carbon in coal fly ash. Energy & Fuels 15, 1414–1417.

Gray, M.L., Champagne, K.J., Soong, Y., Killmeyer, R.P., Maroto-Valer, M.M., Andrésen, J.M., Ciocco, M.V., Zandhuis, P.H., 2002. Physical cleaning of high carbon fly ash. Fuel Processing Technology 76, 11–21.

Heidrich, C., Feuerborn, H., Weir, A., 2013. Coal combustion products: a global perspective. Paper presented at the 2013 World of Coal Ash (WOCA), Lexington, KY, 22–25 April 2013. https://www.flyash.info/

Hurt, R.H., Gibbins, J.R., 1995. Residual carbon from pulverized coal fired boilers: 1. Size distribution and combustion reactivity. Fuel 74(4), 471–480.

International Organization for Standardization (ISO), 2009. Methods for the Petrographic Analysis of Coals. Part 2: Methods of Preparing Coal Samples. ISO 7404-2. ISO, Geneva, Switzerland.

International Organization for Standardization (ISO), 2016. Hard Coal and Coke—Mechanical Sampling. Part 2: Coal—Sampling from Moving Streams. ISO 13909-2. ISO, Geneva, Switzerland.

Külaots, I., Hurt, R.H., Suuberg, E.M., 2004. Size distribution of unburned carbon in coal fly ash and its implications. Fuel 83, 223–230.

Lu, Y., Rostam-Abadi, M., Chang, R., Richardson, C., Paradis, J., 2007. Characteristics of fly ashes from full-scale coal-fired power plants and their relationship to mercury adsorption. Energy & Fuels 21, 2112–2120.

Maroto-Valer, M.M., Taulbee, D.N., Hower, J.C., 1999. Novel separation of the differing forms of unburned carbon present in fly ash using density gradient centrifugation. Energy & Fuels 13, 947–953.

Matjie, R.H., Ginster, M., Van Alphen, C., Sobiecki, A., 2005. Detailed characterisation of Sasol ashes. Paper presented at the 2005 World of Coal Ash (WOCA), Lexington, KY, 11–15 April 2005. https://www.flyash.info/

Matjie, R.H., Li, Z., Ward, C.R., French, D., 2008. Chemical composition of glass and crystalline phases in coarse coal gasification ash. Fuel 87, 857–869.

McMillan, K., Campbell, Q.P., Le Roux, M., Wagner, N., Dorland, H.C., 2015. Composition, component size, fracture patterns and product liberation—washability behaviour of coals from different coalfields of the

world. In: Proceedings of the South African Coal Processing Society Conference, Secunda, South Africa, 25–27 August 2015 (De Korte, J., ed.). South African Coal Processing Society, Secunda.

Mohebbi, M., Rajabipour, F., Scheetz, B.E., 2015. Reliability of loss on ignition (LOI) test for determining the unburned carbon content in fly ash. Paper presented at the 2015 World of Coal Ash (WOCA), Nashville, TN, 5–7 May 2015. https://www.flyash.info/

Pierson, H.O., 1993. Handbook of Carbon, Graphite, Diamond and Fullerenes—Properties, Processing and Applications, 1st ed. Noyes Publications, Park Ridge, NJ, 399 pp.

Reynolds-Clausen, K., Singh, N., 2017. South Africa's power producer's revised Coal Ash Strategy and Implementation Progress. Paper presented at the 2017 World of Coal Ash (WOCA), Lexington, KY, 9–11 May 2017. https://www.flyash.info/

Soong, Y., Link, T.A., Schoffstall, M.R., Turčániová, L., Baláž, P., Marchant, S., Schehl, R.R., 1998. Triboelectrostatic separation of mineral matter from Slovakian coals. Acta Montanistica Slovaca 3, 393–400.

Soong, Y., Schoffstall, M.R., Gray, M.L., Knoer, J.P., Champagne, K.J., Jones, R.J., Fauth, D.J., 2002. Dry beneficiation of high loss-on-ignition fly ash. Separation and Purification Technology 26, 177–184.

Valentim, B., Shreya, N., Paul, B., Gomes, C.S., Sant'Ovaia, H., Guedes, A., Ribeiro, J., Flores, D., Pinho, S., Suárez-Ruiz, I., Ward, C.R., 2016. Characteristics of ferrospheres in fly ashes derived from Bokaro and Jharia (Jharkand, India) coals. International Journal of Coal Geology 153, 52–74.

Wagner, N.J., Malumbazo, N., Falcon, R.M.S., 2018. Southern African Coals and Carbons—Definitions and Applications of Organic Petrology, 1st ed. Struik Nature, Cape Town, South Africa, 248 pp.